

Article

Single-Crystal X-ray Diffraction Analysis of Inclusion Complexes of Triflate-Functionalized Pillar[5]arenes with 1,4-Dibromobutane and n-Hexane Guests

Mickey Vinodh, Shaima G. Alshammari and Talal F. Al-Azemi *

Department of Chemistry, Kuwait University, P.O. Box 5969, Kuwait City 13060, Kuwait

* Correspondence: t.alazemi@ku.edu.kw

Abstract: Herein, we report the single-crystal X-ray diffraction analysis of supramolecular host–guest systems based on triflate-functionalized pillar[5]arenes and 1,4-dibromobutane or *n*-hexane. The guest molecule was stabilized inside the pillar[5]arene cavity by C–H···π and C–H···O interactions. These inclusion complexes were further self-assembled into supramolecular networks by various non-bonding interactions such as C–H···O, C–H···F, Br···Br, F···F, etc. The intermolecular interactions present in these systems were investigated in detail. One of the supramolecular systems analyzed in this study exhibited intermolecular F···F interactions which were operative between the adjacent pillararene rims. It was observed that the type of guest molecule considerably influenced the mutual interactions of pillararene macrocycles and their networking pattern in the crystal. The inclusion complexes were further studied by Hirshfeld surface analysis which not only provided a visual representation of the intermolecular interactions experienced by the systems but gave a quantitative account of these various interactions.

Keywords: triflate-functionalized pillar[5]arene; inclusion complexes; supramolecular assembly; F···F interactions; Hirshfeld surface analysis



Citation: Vinodh, M.; Alshammari, S.G.; Al-Azemi, T.F. Single-Crystal X-ray Diffraction Analysis of Inclusion Complexes of Triflate-Functionalized Pillar[5]arenes with 1,4-Dibromobutane and *n*-Hexane Guests. *Crystals* **2023**, *13*, 593. <https://doi.org/10.3390/crust13040593>

Academic Editor: Ana M. Garcia-Deibe

Received: 26 February 2023

Revised: 19 March 2023

Accepted: 20 March 2023

Published: 31 March 2023



Copyright: © 2023 by the authors. Licensee MDPI, Basel, Switzerland. This article is an open access article distributed under the terms and conditions of the Creative Commons Attribution (CC BY) license (<https://creativecommons.org/licenses/by/4.0/>).

1. Introduction

Pillararene-based macrocycles are gaining considerable importance in contemporary research due to their peculiar structural properties and π-rich deep cavities which enable them to encapsulate a variety of small guest species [1–5]. Pillararene systems containing substituted halogen atoms in their outer rims are of especial interest in the field of supramolecular chemistry because these types of halogen-containing macrocycles can self-assemble into a supramolecular network by halogen–halogen and/or halogen–hydrogen interactions. Supramolecular host–guest systems constructed by such halogen-based non-covalent interactions have drawn considerable interest in recent years [6–20]. Heavier halogens, particularly bromo and iodo derivatives, have been widely utilized in the assembly of such systems because they exhibit electrophilic characteristics and can interact with electron-pair-donating heteroatoms (O, N, S) or anions because of the anisotropic distribution of the electrostatic potential around the atomic center. However, supramolecular systems mediated by F···F interactions are not commonly encountered [20,21], especially for macrocyclic systems such as pillararenes.

Pillar[n]arenes possess excellent guest encapsulation and molecular recognition properties, making them ideal building blocks for the preparation of supramolecular polymers [6,7]. A novel supramolecular linear polymer system based on the guest encapsulation of 1,4-dibromobutane by permethylated-pillar[5]arenes both in solution and in a solid state has been reported previously [6,7]. The crystal structure of the obtained inclusion complex shows that the guest molecule is tightly stabilized inside the pillar[5]arene cavity by C–H···π and C–H···O interactions. The novel linear supramolecular assembly is formed by the bonding between the bromine atoms of encapsulated dibromobutane

molecules located inside the pillar[5]arene cavity with the adjacent inclusion complex, through Br···Br interactions.

In this work, we report the co-crystal structures of pillararene systems conjugated with mono- and di-substituted triflate moieties with dibromobutane and *n*-hexane guests. The detailed comparison study provides insight on the effect of halogen-containing guest molecules on the supramolecular behavior of these inclusion systems. The structural features and supramolecular host–guest interactions of these co-crystalline systems (Pil_TF1_ButBr2, Pil_TF1_Hex, Pil_TF2_ButBr2 and Pil_TF2_Hex) are addressed and discussed.

2. Materials and Methods

The single-crystal data collection was made either using the Bruker X8 prospector (Germany) diffractometer with Cu-K α radiation or the Rigaku Rapid II (Japan) diffractometer with Mo-K α radiation. In the former case, the reflection frames were integrated with the Bruker SAINT Software package using a narrow-frame algorithm. Finally, the structure was solved using the Bruker SHELXTL software package and refined using SHELXL-2017/1. The data collected using the Rigaku diffractometer were processed using the ‘Crystalclear’ software package. The structure was then solved by direct methods using the Crystal-Structure crystallographic software package and the refinement was performed using SHELXL-2017/1. Nuclear magnetic resonance (NMR) spectroscopy was conducted using the Bruker DPX Avance 400 MHz (Germany) spectrometer. Electron impact ionization (EI) mass spectrometry was performed using the Thermo Scientific DFS High Resolution GC/MS (Germany) mass spectrometer. 1-(1,4-ditriflate)-2,3,4,5-dimethoxy pillar[5]arene (**Pil-TF2**) was synthesized based on the previously reported procedure [22].

2.1. Synthesis of 1-(1-triflate-4-methoxy)-2,3,4,5-dimethoxy Pillar[5]arene (Pil-TF1)

To a solution of 1-(1-hydroxy-4-methoxy)-2,3,4,5-dimethoxy pillar[5]arene [23] (147 mg, 0.2 mmol) in CH₂Cl₂ (30 mL), pyridine (18 μ L, 0.22 mmol) was added and the mixture was stirred at 0 °C for 10 min. Triflic anhydride (34 μ L, 0.2 mmol) was then added at 0 °C, and the mixture was stirred at room temperature for 4 h. The solution was washed with aqueous HCl solution (1.0 M, 3 × 30 mL), solvent was removed under reduced pressure and the residue was purified using column chromatography to afford the desired product **Pil-TF1** as a white solid (Yield 121 mg, 70%). ¹H NMR (400 MHz, CDCl₃), δ : 3.69 (m, 27H), 3.80 (m, 8H), 3.87 (s, 2H), 6.75 (m, 2H), 6.80 (m, 6H), 6.87 (s, 1H), 7.15 (s, 1H). ¹³C NMR (100 MHz, CDCl₃), δ : 29.5, 29.6, 29.6, 30.7, 52.4, 55.5, 55.6, 55.6, 55.8, 55.9, 55.9, 56.0, 113.6, 113.7, 113.7, 114.0, 114.0, 114.1, 114.1, 114.2, 123.1, 126.0, 127.0, 128.3, 128.5, 128.5, 128.9, 129.3, 130.0, 132.5, 141.1, 150.6, 150.8, 150.9, 150.9, 151.0, 156.1. HRMS: (m/z): calculated for [M]⁺: 868.2740 (for C₄₅H₄₇O₁₂F₃S); found 868.2737.

2.2. Preparation of Single Crystals for X-ray Diffraction

Suitable single crystals of the inclusion complexes **Pil-TF2_ButBr2**, **Pil-TF2_Hex**, **Pil-TF1_ButBr2** and **Pil-TF1_Hex** were grown using the slow solvent evaporation method from dichloromethane/1,4 dibromobutane (1 mL, 90: 10; v/v) or dichloromethane/*n*-hexane mixtures. All non-hydrogen atoms were refined anisotropically and hydrogen atoms were refined using the riding model. The crystallographic data for structures reported in this paper have been deposited at the Cambridge Crystallographic Data Centre (CCDC 2244581-2244584).

3. Results and Discussion

3.1. Crystal Structures of Triflate-Functionalized Pillar[5]arenes with 1,4-dibromobutane or *n*-hexane

The crystal structures of di-substituted triflate pillar[5]arene obtained from the solution containing 1,4-dibromobutane (**Pil_TF2_ButBr2**) and those obtained from the solution containing *n*-hexane (**Pil_TF2_Hex**) are depicted in Figure 1 and their crystallographic features are given in Table 1. As expected, both **Pil_TF2_ButBr2** and **Pil_TF2_Hex** crystals

constitute pillar[5]arene macrocycle encapsulated with either dibromobutane or n-hexane in its cavity. The dibromobutane present in the cavity of Pil_{TF2} exhibits positional disorder and hence the crystal refinement could be made possible by assigning its location at two different sites in the cavity. In Figure 1, the position of those dibromobutanes with higher occupancy (60%) has been shown. Furthermore, one of the triflate sites in this crystal exhibited positional disorder with respect to the corresponding sulfur and two attached oxygen atoms, and this too is refined over two sites with 70% and 30% occupancies, respectively. Moreover, in the case of Pil_{TF2_Hex}, one of the triflate sites exhibited positional disorder with respect to the corresponding sulfur atom and thus performed refinement over two sites (with around 63% and 37% occupancies, respectively).

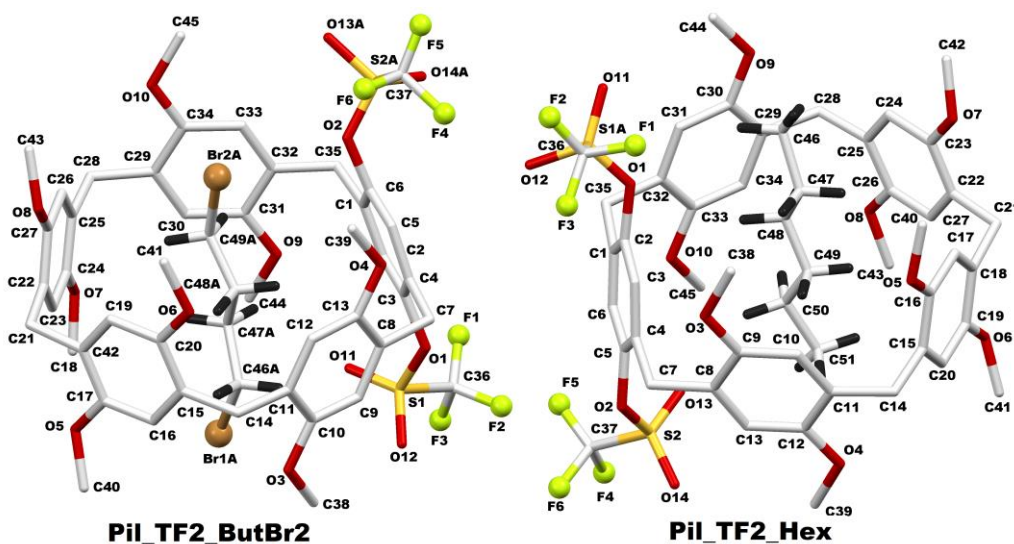


Figure 1. Crystal structure of Pil_{TF2}_ButBr₂ and Pil_{TF2}_Hex (hydrogen atoms on the pillar[5]arene ring have been hidden for clarity).

Table 1. Summary on the nature and various crystallographic parameters of Pil_{TF2}_ButBr₂ and Pil_{TF2}_Hex.

Crystal Sample	Pil-F2-ButBr2	Pil-TF2-Hexane
Chemical formula	C49H52Br2F6O14S2	C51H58F6O14S2
Mr	1202.84	1073.09
Crystal system, space group	Mono-clinic, P21/c	Mono-clinic, P21/c
Temperature (K)	150	150
a, b, c (Å)	18.4426 (10), 18.580 (1), 15.8047 (7)	18.1057 (13), 18.7444 (14), 15.8021 (11)
α, β, γ (°)	98.962 (7)	99.305 (4)
V (Å ³)	5349.6 (5)	5292.4 (7)
Z	4	4
Radiation type	Mo K α	Cu K α
μ (mm ⁻¹)	1.68	1.65
Crystal size (mm)	0.20 × 0.20 × 0.16	0.21 × 0.18 × 0.17
Diffractometer	Rigaku R-AXIS RAPID	Bruker APEX-II CCD Multi-scan
Absorption correction	Multi-scan ABSCOR (Rigaku, 1995)	SADABS2016/2—Bruker AXS area detector scaling and absorption correction
Tmin, T _{max}	0.72, 0.79	0.71, 0.78
No. of measured, independent and observed [I > 2σ(I)] reflections	37,489, 9339, 5489	40,804, 8995, 4711

Table 1. Cont.

Crystal Sample	Pil-F2-ButBr2	Pil-TF2-Hexane
Rint	0.049	0.098
(sin θ/λ)max (\AA^{-1})	0.595	0.595
R[F2 > 2 σ (F2)], wR(F2), S	0.095, 0.321, 1.04	0.099, 0.348, 1.04
No. of reflections	9339	8995
No. of parameters	741	676
No. of restraints	287	89
H-atom treatment	Constrained	Constrained
$\Delta\rho_{\text{max}}, \Delta\rho_{\text{min}}$ ($e \text{\AA}^{-3}$)	1.40, -0.65	0.74, -0.63

The crystal structure of mono-substituted triflate pillar[5]arene obtained from the solution containing 1,4 dibromobutane (**Pil_TF1_ButBr2**) and those obtained from the solution containing n-hexane (**Pil_TF1_Hex**) are shown in Figure 2. The crystallographic parameters of both these crystals are provided in Table 2. As in the case of its ditriflate analogue, both **Pil_TF1_ButBr2** and **Pil_TF1_Hex** crystals comprise pillar[5]arene macrocycles along with either dibromobutane or n-hexane guests in the cavity. The dibromobutane present in the cavity of **Pil_TF1** too exhibits positional disorder as in the case of **Pil_TF1_ButBr2** and hence refined over two different sites in the pillararene cavity with 53% and 47% occupancies, respectively. **Pil_TF1_Hex** also exhibited positional disorder at one of sulfur atoms belonging to the triflate site with around 57% and 43% occupancies, respectively.

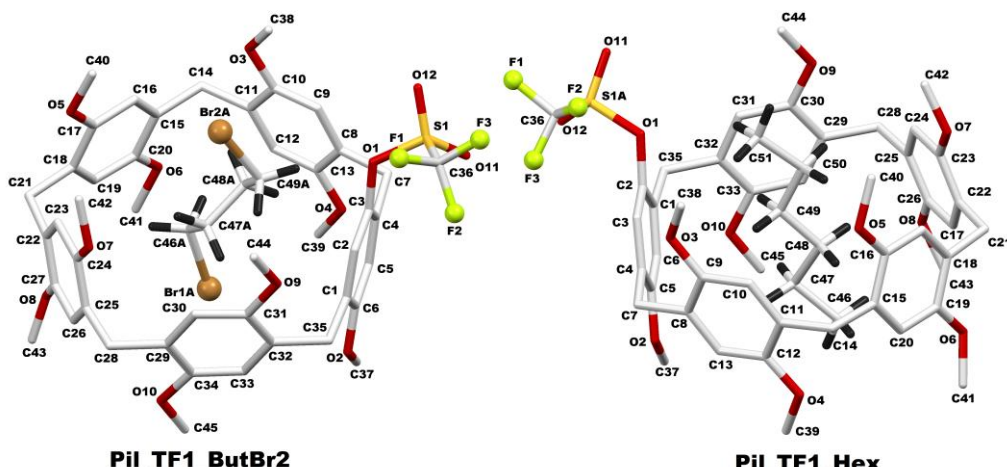


Figure 2. Crystal structure of **Pil_TF1_ButBr2** and **Pil_TF1_Hex** (hydrogen atoms on the pillar[5]arene ring have been hidden for clarity).

Table 2. Summary on the nature and various crystallographic parameters of **Pil_TF1_ButBr2** and **Pil_TF1_Hex**.

Crystal Sample	Pil-F1-ButBr2	Pil-TF1-Hexane
Chemical formula	$C_{49}H_{55}Br_2F_3O_{12}S$	$C_{51}H_{61}F_3O_{12}S$
M_r	1084.81	955.05
Crystal system, space group	Orthorhombic, $Pna2_1$	Orthorhombic, $Pna2_1$
Temperature (K)	150	150
a, b, c (\AA)	36.345 (4), 12.1749 (13), 11.4616 (13)	36.5154 (14), 12.1508 (5), 11.4520 (4)
V (\AA^3)	5071.7 (10)	5081.2 (3)
Z	4	4
Radiation type	$Cu K\alpha$	$Cu K\alpha$

Table 2. Cont.

Crystal Sample	Pil-F1-ButBr2	Pil-TF1-Hexane
μ (mm^{-1})	3.01	1.16
Crystal size (mm)	$0.22 \times 0.21 \times 0.18$	$0.21 \times 0.17 \times 0.12$
Diffractometer	Bruker APEX-II CCD	Bruker APEX-II CCD
	Multi-scan	Multi-scan
Absorption correction	SADABS2016/2—Bruker AXS area detector scaling and absorption correction	SADABS2016/2—Bruker AXS area detector scaling and absorption correction
T_{\min}, T_{\max}	0.57, 0.63	0.79, 0.84
No. of measured, independent and observed [$I > 2\sigma(I)$] reflections	28,160, 7434, 6869	32,409, 7710, 7322
R_{int}	0.057	0.038
$(\sin \theta / \lambda)_{\max}$ (\AA^{-1})	0.596	0.595
$R[F^2 > 2\sigma(F^2)]$, $wR(F^2)$, S	0.116, 0.329, 1.51	0.073, 0.216, 1.00
No. of reflections	7434	7710
No. of parameters	660	615
No. of restraints	244	127
H-atom treatment	Constrained	H-atom parameters constrained
$\Delta\rho_{\max}, \Delta\rho_{\min}$ ($e \text{\AA}^{-3}$)	0.74, -1.27	0.99, -0.69

3.2. Host–Guest Inclusion Complexes of Di- and Mono-Substituted Triflate Pillar[5]arenes with 1,4-dibromobutane and *n*-hexane

The crystal structures of all the four pillararene systems show that 1,4-dibromobutane/*n*-hexane guest species are threaded inside the pillararene cavity forming 1:1 inclusion complex. It can be seen that almost all H-atoms of the guest molecules are capable of involving bonding with a pillararene ring either via C-H····O or C-H···· π non-bonding interactions. The nature of these various non-bonding interactions is depicted in Figures 3 and 4 and their quantitative details are provided in the Supporting Information.

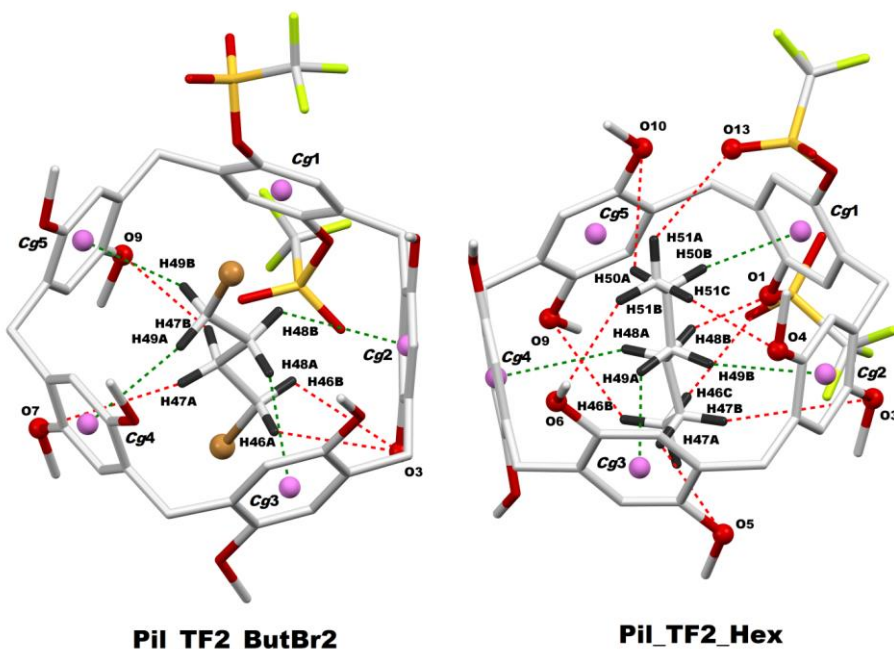


Figure 3. Possible host–guest interactions between pillar[5]arene ring and guest molecule in Pil_TF2_ButBr2 and Pil_TF2_Hex systems. Cg1–Cg5 are the centroids of the C1–C6, C8–C13, C15–C20, C22–C27 and C29–C34 rings, respectively. (Hydrogen atoms on the pillar[5]arene ring have been hidden for clarity).

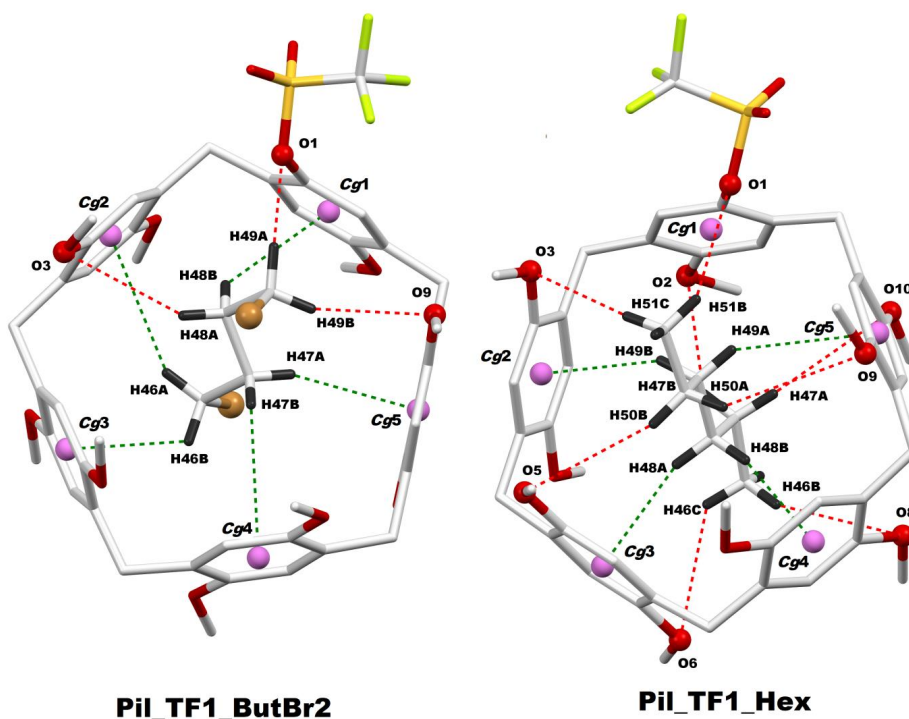


Figure 4. Possible host–guest interactions between pillar[5]arene ring and guest molecule in Pil_TF1_ButBr2 and Pil_TF1_Hex systems. Cg1–Cg5 are the centroids of the C1–C6, C8–C13, C15–C20, C22–C27 and C29–C34 rings, respectively. (Hydrogen atoms on the pillar[5]arene ring have been hidden for clarity).

3.3. Intermolecular Non-Bonding Interactions among Pil_TF2 Crystals

The 1:1 inclusion complexes of triflate-substituted pillar[5]arenes and dibromobutane/n-hexane are capable of involving many non-bonding interactions in their crystal network. The non-bonding interactions (less than the van del Waals range) experienced by Pil_TF2_ButBr2 and Pil_TF2_Hex from their immediate neighbors are shown in Figure 5. In the case of Pil_TF2_Hex crystals, it can be seen that the intermolecular non-bonding interactions included C-H···F and C-H···O types. However, in the case of Pil_TF2_ButBr2 crystals, the range of these non-bonding interactions extends further to very interesting and highly significant F···F and Br···Br interactions in addition to C-H···F and C-H···O bonds (Figure 5).

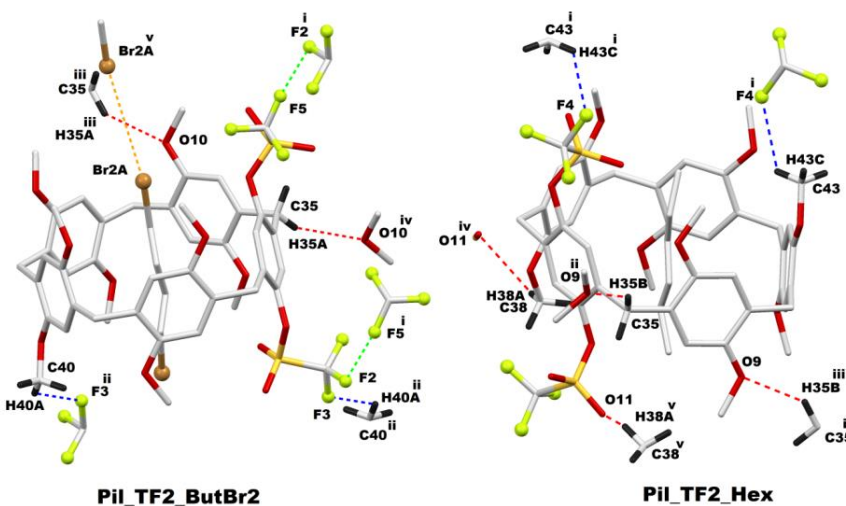


Figure 5. Possible intermolecular interactions between Pil_TF2_ButBr2 and Pil_TF2_Hex systems in crystal network with adjacent pillar[5]arene molecules of different symmetries. (Different types of interactions are demonstrated by different colored lines: Br···Br—brown; O···H—red; F···F—green)

and F···H—blue.) Symmetry code for **Pil_TF2_ButBr2**: (i) $-x, 1-y, 1-z$; (ii) $1-x, 1-y, 1-z$; (iii) $x, 1.5-y, -1/2+z$; (iv) $x, 1.5-y, 1/2+z$ and (v) $-x, 1-y, -z$; symmetry code for **Pil_TF2_Hex**: (i) $-x, 1-y, 1-z$; (ii) $x, \frac{1}{2}-y, -1/2+z$; (iii) $x, \frac{1}{2}-y, \frac{1}{2}+z$; (iv) $1-x, \frac{1}{2}+y, 1.5-z$ and (v) $1-x, -1/2+y, 1.5-z$.

The quantitative details of all these non-bonding interactions are provided in Tables 3 and 4 where both interaction distances and corresponding angles are given. Due to the positional disorder of the dibromobutane guest in the crystals, it is not possible to provide an accurate quantification of Br···Br interactions in the crystal and hence its values are excluded in Table 3. It is evident from Table 3 that F···F interaction distance in **Pil_TF2_ButBr2** crystals is 2.753(8) Å, which is ca. 6% shorter than the sum of the respective van der Waals atomic radii (2.94 Å). A comprehensive work on various aspects of C-F···F-C and C-H···F-C interactions in organic crystals was reported by Levina et al. [20]. Through various experimental and theoretical calculations in their work, the authors reported that the presence of C-F···F-C interactions in crystals could be confirmed if F···F distances are less than 2.94 Å. Therefore, the F···F bond length of 2.753(8) Å shown by the **Pil_TF2_ButBr2** crystal reveals that these pillararene molecules are held together to form a supramolecular network by a great contribution of the rare F···F mediated interactions.

Table 3. Intermolecular non-bonding interactions (shorter than the sum of van der Walls radii) in the **Pil_TF2_ButBr2** crystals (Å, °).

A-B···C	A-B	B···C	A···C	A-B···C
C36-F2···F5 ⁱ	1.31(1)	2.753(8)	3.61(1)	121.06(6)
C37-F5···F2 ⁱ	1.27(1)	2.753(8)	3.88(1)	147.3(8)
C40-H40A···F3 ⁱⁱ	0.96	2.588	3.232(9)	124.6
C36-F3···H40A ⁱⁱ	1.32(1)	2.588	3.559	128.0
C34-O10···H35A ⁱⁱⁱ	1.382(6)	2.546	3.760	144.8
C35-H35A···O10 ^{iv}	0.970	2.546	3.377(6)	143.7

Symmetry code: (i) $-x, 1-y, 1-z$; (ii) $1-x, 1-y, 1-z$; (iii) $x, 1.5-y, -1/2+z$; (iv) $x, 1.5-y, 1/2+z$.

Table 4. Intermolecular non-bonding interactions (shorter than the sum of van der Walls radii) in the **Pil_TF2_Hex** crystals (Å, °).

A-B···C	A-B	B···C	A···C	A-B···C
C40-H43C···F4 ⁱ	0.96	2.631	3.31(1)	127.6
C37-F4···H43C ⁱ	1.45(1)	2.631	3.52	116.6
C35-H35B···O9 ⁱⁱ	0.97	2.563	3.381(6)	142.2
C30-O9···H35B ⁱⁱⁱ	1.389(6)	2.563	3.770	143.4
C38-H38A···O11 ^{iv}	0.961	2.719	3.395(9)	128.0
S1A-O11···H38A ^v	1.41(1)	2.719	3.33	103.1

Symmetry code: (i) $-x, 1-y, 1-z$; (ii) $x, 1/2-y, -1/2+z$; (iii) $x, 1/2-y, 1/2+z$; (iv) $1-x, 1/2+y, 1.5-z$; (v) $1-x, -1/2+y, 1.5-z$.

A close observation of the **Pil_TF2_ButBr2** and **Pil_TF2_Hex** crystals reveals that both these molecules have similar packing in the crystal. A short section of their crystal network (comprising four pillar[5]arene units) is given in Figure 6 which shows that the triflate fractions of every two adjacent pillar[5]arene molecules are close to each other in both crystals. In the case of the **Pil_TF2_Hex** crystals, the packing is in such a manner that the closest F···F distance between two adjacent pillar[5]arennes is 2.941 Å, which is almost equal to the sum of their respective van der Waals atomic radii. At the same time, in the case of **Pil_TF2_ButBr2**, the closest F···F distance, as mentioned earlier, is found to be reduced significantly to 2.753(8) Å, thereby enabling efficient F···F interactions in the crystal. The reason for this remarkable difference in these two crystal samples is the presence of different types of guest molecules encapsulated within them. When dibromobutane is encapsulated in the **Pil_TF2** crystal, appreciable Br···Br interaction between two adjacent dibromobutanes occurs, which in turn causes the two triflate fragments to move close to

each other, enabling $\text{F}\cdots\text{F}$ interactions. Therefore, it is clear that the nature of the guest molecule influences the supramolecular characteristics of the host molecule and proper selection of such host–guest combinations can generate interesting functional systems.

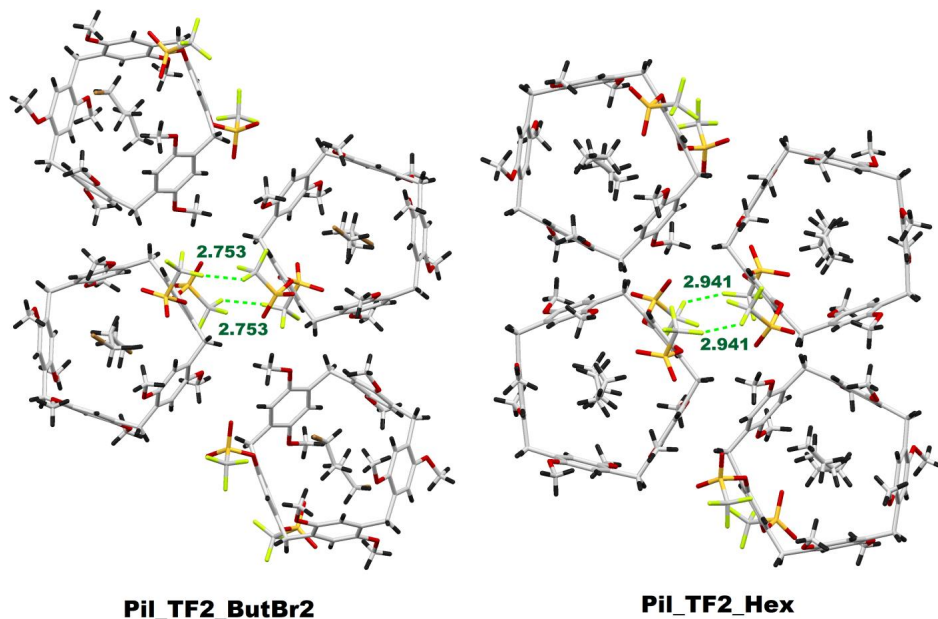


Figure 6. Comparison between $\text{F}\cdots\text{F}$ interaction distances in **Pil_TF2_ButBr2** and **Pil_TF2_Hex** crystals.

The two-dimensional packing of both **Pil_TF2_Hex** and **Pil_TF2_ButBr2** crystals is provided in Figures 7 and 8, respectively, which provided a clear demonstration of how different $\text{F}\cdots\text{F}$, $\text{F}\cdots\text{H}$ and $\text{Br}\cdots\text{Br}$ occurred in the crystal network and the impact of these interactions on the crystal packing. In the case of **Pil_TF2_Hex**, the pilla[5]arene units are arranged linearly in different rows. In this linear assembly of each row, two adjacent pillar[5]arene molecules are co-facially interacted with by two $\text{F}\cdots\text{H}$ bonds, forming a dimeric unit. However, there is no significant interaction involving $\text{F}\cdots\text{F}$, $\text{F}\cdots\text{H}$ bonds between any dimer and its adjacent counterpart in the linear assembly or between two pillar[5]arenes in different rows. In **Pil_TF2_ButBr2**, crystals show significant influences of $\text{F}\cdots\text{F}$, $\text{F}\cdots\text{H}$ and $\text{Br}\cdots\text{Br}$ interactions. In addition, the pillar[5]arene units are arranged linearly as co-facial dimers in different rows by $\text{F}\cdots\text{H}$ bonds as in the case of **Pil_TF2_Hex**. Moreover, to these $\text{F}\cdots\text{H}$ bonds between the two adjacent pillar[5]arenes, there are $\text{Br}\cdots\text{Br}$ interactions between two dibromobutane molecules which are encapsulated by the pillar[5]arenes in the linear chain. The interesting feature of this $\text{Br}\cdots\text{Br}$ interaction is not found between the guest molecules of co-facial dimeric units in the pillar[5]arene linear assembly but between two pillar[5]arenes of adjacent dimers. The combined effect of these two types of interaction, namely $\text{F}\cdots\text{H}$ and $\text{Br}\cdots\text{Br}$, is that all pillar[5]arene-dibromobutane host-guest systems in the **Pil_TF2_ButBr2** crystal are connected to one another along the linear assembly making a chain of pillar[5]arenes in the network. Furthermore, pillararene in each linear chain is bonded to a neighboring pillararene of a different row through $\text{F}\cdots\text{F}$ interactions at two macrocyclic sites. It should be noted that alternate **Pil_TF2** molecules in the linear assembly engage these $\text{F}\cdots\text{F}$ interactions towards pillararenes of the same rows and the other alternate **Pil_TF2** molecules interact with the macrocycles lying on the rows on the opposite side. As a result, the pillararene self-assembly in the **Pil_TF2_ButBr2** crystal could be considered as a linear propagation of a host–guest species at different rows mediated by the combined effect of $\text{F}\cdots\text{H}$ and $\text{Br}\cdots\text{Br}$ interactions, along with efficient $\text{F}\cdots\text{F}$ interactions propagating sideways with respect to this linear chain in an alternate frequency. Although both **Pil_TF2_Hex** and **Pil_TF2_ButBr2** crystals show similar patterns in their networks, the latter crystals are much more significant from a supramolecular

point of view. This difference signifies the effect of guest molecules in the supramolecular characteristics of the host–guest systems.

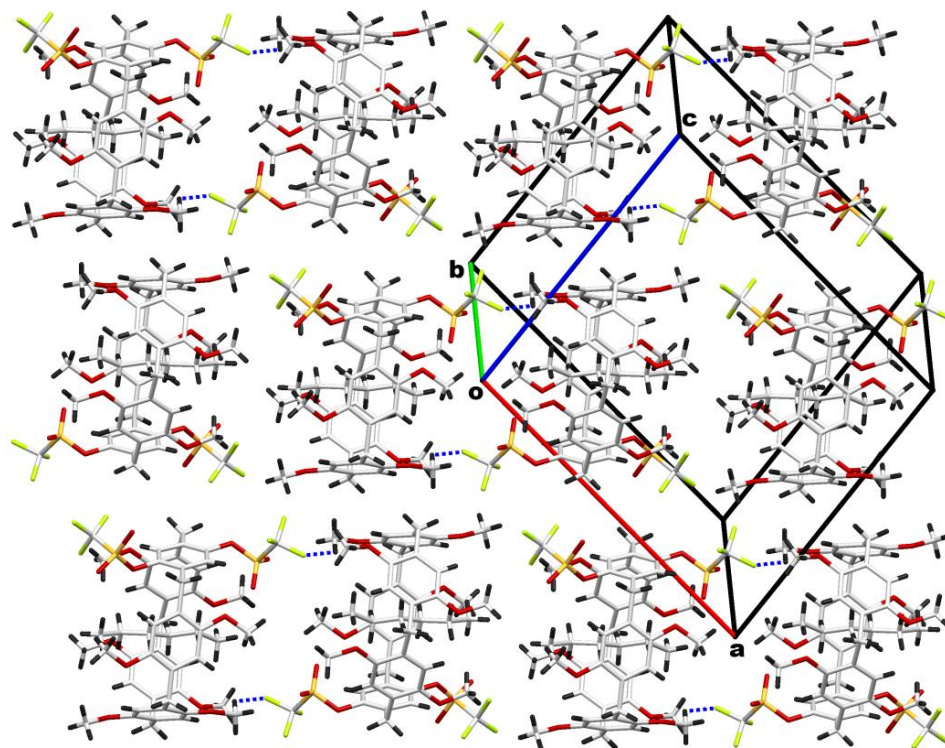


Figure 7. Crystal network of Pil_TF2_Hex host–guest system showing different rows of linear pillar[5]arne arrays enabled by F···H interactions. The F···H interactions are in such a way that pillar[5]arenes exit as co-facial dimers in the linear assembly.

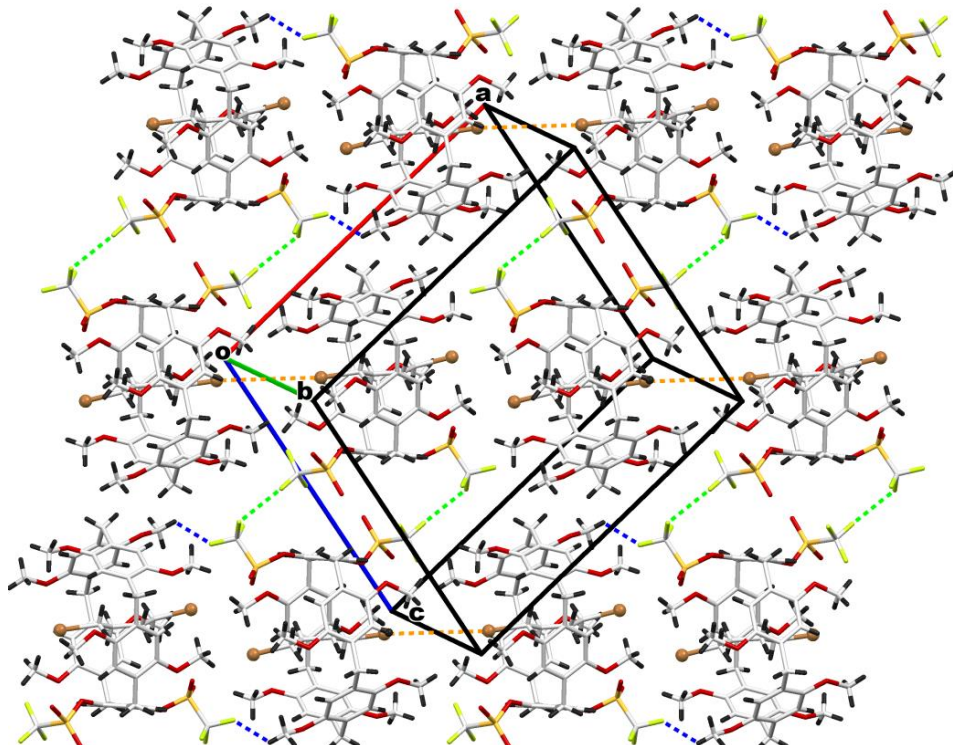


Figure 8. Crystal network of Pil_TF2_ButBr2 host–guest system showing different rows of linear pillararene arrays enabled by Br···Br (brown), F···F (green) and F···H (blue) interactions.

In **Pil_TF1** crystals, the guest molecule contributes significantly to the intermolecular interactions. The 1:1 inclusion complexes of **Pil_TF1** and 1,4-dibromobutane/*n*-hexane are capable of involving non-bonding interactions with immediate neighbors in their crystal networks, which are given in Figure 9 (which shows those that are less than the van der Waals range).

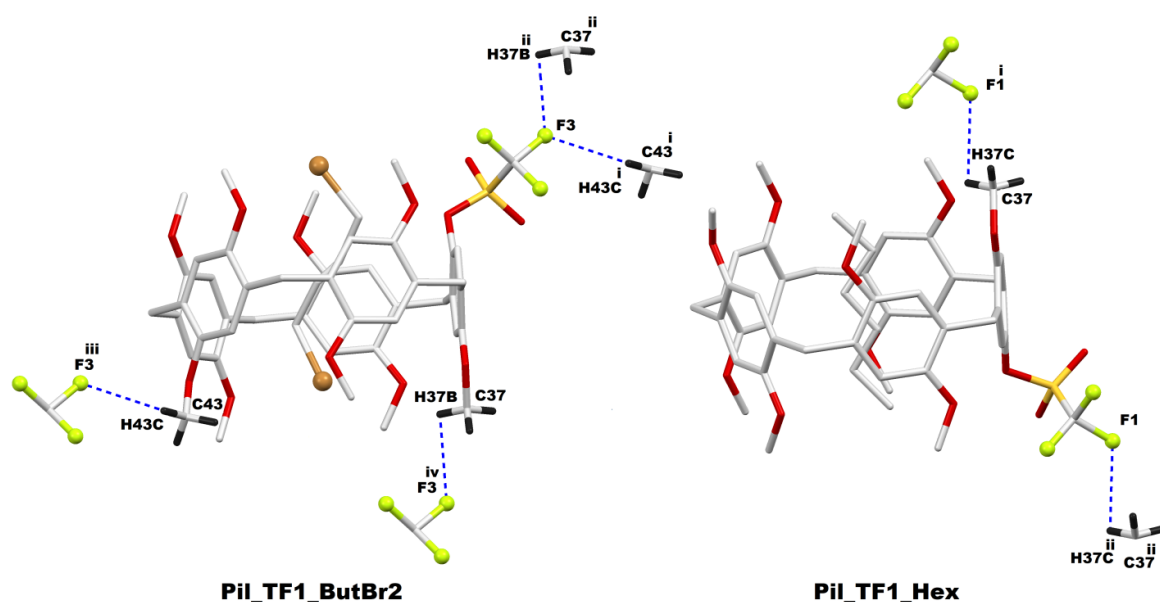


Figure 9. Intermolecular interactions between **Pil_TF1_ButBr2** and **Pil_TF1_Hex** systems in crystal network with adjacent pillararene molecules of different symmetries. Symmetry code for **Pil_TF1_ButBr2**: (i) $x, 1+y, 1+z$; (ii) $x, y, 1+z$; (iii) $x, -1+y, -1+z$ and (iv) $x, y, -1+z$; symmetry code for **Pil_TF1_Hex**: (i) $x, y, -1+z$ and (ii) $x, y, 1+z$.

In both **Pil_TF1_Hex** and **Pil_TF1_ButBr2** crystals, there are efficient C-H \cdots F interactions. However, in the latter case, where the dibromobutane is encapsulated, the total number of such C-H \cdots F interactions experienced by a single pillar[5]arene unit is doubled when compared to its hexane encapsulated counterpart as shown in Figure 9. The quantitative details of all these C-H \cdots F non-bonding interactions exhibited by **Pil_TF1_ButBr2** and **Pil_TF1_Hex** crystals are provided in the Supporting Information where both interaction distances and corresponding angles are given.

The crystal network of both **Pil_TF1_Hex** and **Pil_TF1_ButBr2** have similar features with linear assembly of pillar[5]arene units arranged in different arrays. It is interesting to note that in the case of the **Pil_TF1_Hex** crystal, each pillar[5]arene in the linear chain is connected by an F \cdots H bond at both ends (Figure 10). In the case too of the **Pil_TF1_ButBr2** crystal, each pillar[5]arene in the linear chain is connected by an F \cdots H bond at both ends. In addition, there is a sideways interaction through another set of F \cdots H bonds between pillar[5]arennes in different rows, which make it an overall two-dimensionally propagated F \cdots H bond structure, as demonstrated in Figure 11.

It is interesting to note that the mono-triflate upon hexane encapsulation gives a linear chain while di-triflate upon the same guest encapsulation gives a linear assembly with co-facial dimeric units as demonstrated in the Supporting Information.

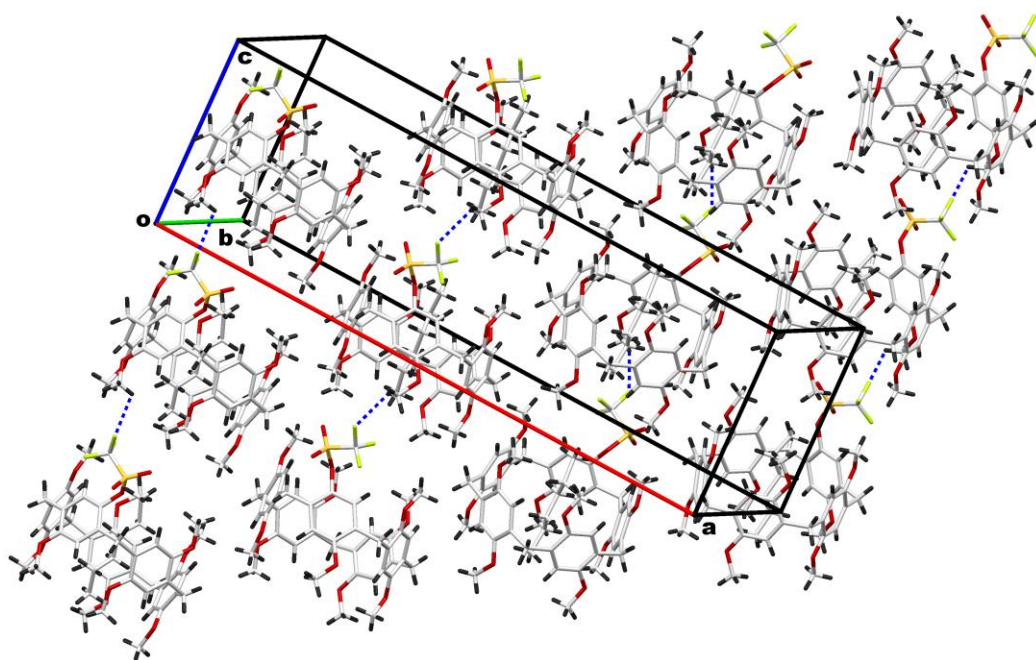


Figure 10. Crystal network of Pil_TF1_Hex host–guest system showing different rows of linear pillar[5]arene chains enabled by $\text{F}\cdots\text{H}$ interactions.

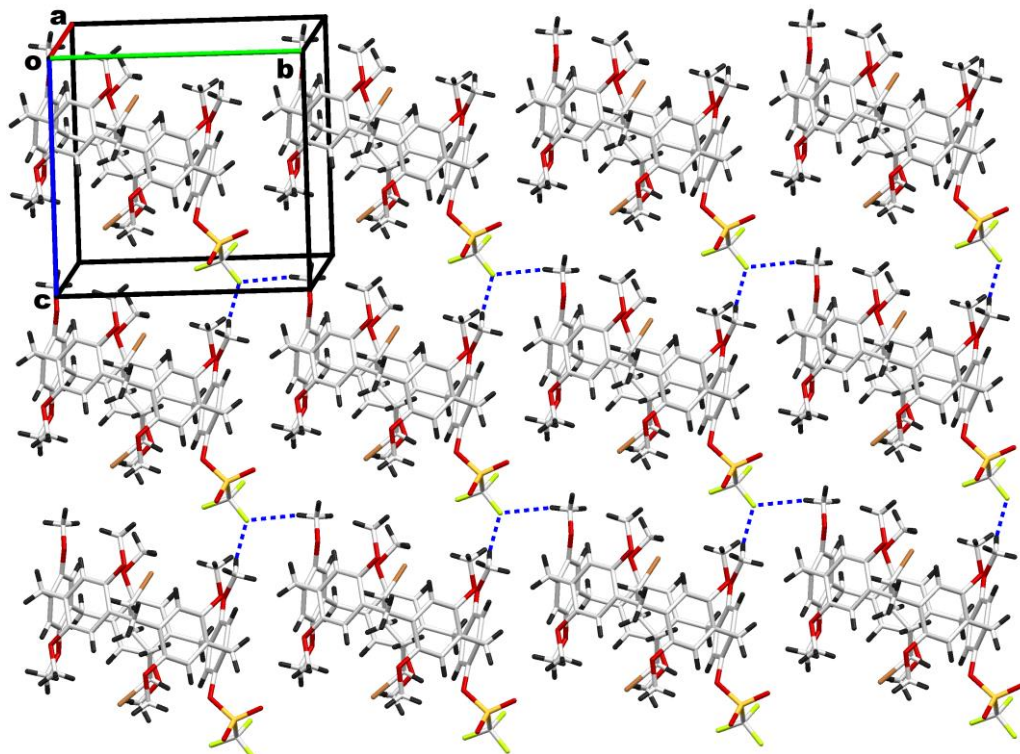


Figure 11. Crystal network of Pil_TF1_ButBr2 host–guest system showing different rows of pillar[5]arene chains enabled by $\text{F}\cdots\text{H}$ interactions. Both linear and sideways interactions present in the system are demonstrated.

3.4. Hirshfeld Surface Analysis of Co-Crystals Constituting Triflate-Functionalized Pillar[5]arenes and 1,4-Dibromobutane/n-Hexane

The non-bonding interactions experienced by triflate-functionalized pillararens discussed in this study were further investigated by Hirshfeld surface analysis. The Hirshfeld surface analysis offers a visual representation of the intermolecular interactions and, thus,

serves as a powerful tool for gaining additional insights into crystal structures [24–26]. There are two main characteristic features in the Hirshfeld surface analysis, namely, 3D dnorm surface images and 2D fingerprint plots. The 3D dnorm surface is helpful for visualizing and analyzing the intermolecular interactions experienced by a species in the crystal. The red colored regions on the Hirshfeld surface indicate the intermolecular contacts shorter than the sum of the relevant van der Waals radii. White regions indicate intermolecular distances close to van der Waals contacts and blue regions are contacts longer than the sum of the respective van der Waals radii. At the same time, the 2D fingerprint plots give a quantitative summarization of the nature and type of various intermolecular contacts experienced by a particular moiety in the crystal. In the present study, the Hirshfeld surface analysis was performed using Crystal Explorer 17.1 [27]. Due to positional disorder, the structures of these crystals were remodeled in this section for the generation of the Hirshfeld surface by choosing only the disordered components of greater occupancy. This is achieved by manually editing the CIF to remove atoms from all the disorder components except the one which is more populated and setting all the atoms to be fully occupied.

The Hirshfeld surface mapped with the dnorm function for **Pil_TF2_ButBr2** clearly shows intense red spots which correspond to the F···F interactions (Figure 12). Other interactions such as H···H, F···H, O···H, C···H and Br···Br could be seen in the surface as faded red spots and white regions. The red areas arising from intermolecular F···F interactions are very intense implying the dominance of these interactions in the crystal. As expected, the appearance of the Hirshfeld surface of **Pil_TF2_Hex** is much different from that of **Pil_TF2_ButBr2** due to a lack of intense F···F intermolecular interactions between them. Some diffused red/white regions in the surface of **Pil_TF2_Hex** dnorm is due to H···H, F···H, C···H or O···H interactions.

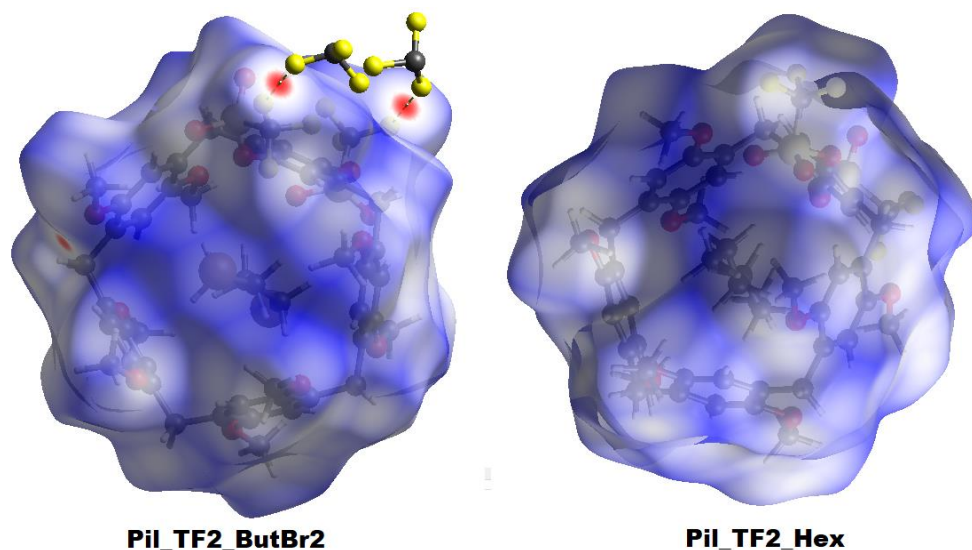


Figure 12. Hirshfeld surfaces (mapped with dnorm) of the **Pil_TF2_ButBr2** and **Pil_TF2_Hex** crystals.

From the 2D fingerprint plots, the major intermolecular interactions in the **Pil_TF2_ButBr2** crystals are H···H (38.7%), F···H (20.1), O···H (17.2%), C···H (11.4%), Br···H (2.2%) and F···F (2.4%). The 2D fingerprint plot shows that the Br···Br interactions in this crystal contribute 0.8% of the total intermolecular interactions, which is significant when considering the fact that only two bromine atoms are present in the asymmetric unit of the crystal. In the case of the **Pil_TF2_Hex** crystal, the major intermolecular interactions corresponding to the 2D fingerprint plots are H···H (42.4%), F···H (21.5), O···H (17.9%), C···H (11.5%) and F···F (1.5%). As expected, all these percentage contributions in the **Pil_TF2_Hex** crystal are higher than those values of **Pil_TF2_ButBr2**, except for the contribution of F···F interactions due to the absence Br-mediated interactions in the former crystals. Even then, the superior contribution of F···F interactions in **Pil_TF2_ButBr2** compared to **Pil_TF2_Hex** is in full

agreement with the observation that the encapsulation of 1,4-dibromobutane by the pillararene promoted F···F bonding, as demonstrated earlier.

As there is no remarkable difference in the non-bonding interactions between the crystal structures, the Hirshfeld surface mapped with the dnorm function for **Pil_TF1_ButBr2** and **Pil_TF1_Hex** exhibited almost similar surface features, which is shown in the Supporting Information. Regarding the quantitative details, the major intermolecular interactions in the **Pil_TF1_ButBr2** crystals based on the 2D fingerprint plots are H···H (48.5%), O···H (16.8%), C···H (14.5%), F···H (12.8%) and Br···H (4.5%). At the same time, the corresponding contributions for **Pil_TF1_Hex** crystals are H···H (52.8%), O···H (17.1%), C···H (14.5%) and F···H (13.4%). It should be noted that the contributions of F···F and Br···Br interactions are insignificant (0.0% and 0.1%, respectively) in the **Pil_TF1_ButBr2** crystals.

4. Conclusions

To conclude, host–guest supramolecular systems based on mono- and di-triflate-functionalized-pillar[5]arene with 1,2-dibromobutane/n-hexane have been developed. Efficient host–guest complexation between the pillararenes and 1,4-dibromobutane and n-hexane has been observed in all these systems. Both mono- and di-functionalized-pillar[5]arens were self-arranged into linear assembly in their crystal upon guest encapsulation by employing various non-bonding interactions such as F···H bonding. However, in one of the supramolecular systems comprising di-functionalized-pillar[5]arens with dibromobutane, highly efficient and useful F···F and Br···Br interactions were observed in the crystal network. This result suggests that these types of fluorine-functionalized pillarane, if subjected to fine tuning by the appropriate selection of guest molecules, could be employed to generate useful functional materials.

Supplementary Materials: The following supporting information can be downloaded at <https://www.mdpi.com/article/10.3390/crust13040593/s1>. Crystallographic tables, Hirshfeld surface figure and Check CIF's.

Author Contributions: All authors contributed equally to this work. The manuscript was written through contributions of all authors. All authors have read and agreed to the published version of the manuscript.

Funding: The support received from Kuwait University (made available through research Grant no. SC08/19), the Graduate School at Kuwait University and the facilities of the RSPU (Grant Nos. GS01/01, GS03/01, GS01/03, GS01/10 and GS03/08) is gratefully acknowledged.

Data Availability Statement: The data presented in this study are available in Supplementary Materials here.

Acknowledgments: The support received from the Kuwait University research sector, the Graduate School at Kuwait University and the facilities of the RSPU is gratefully acknowledged.

Conflicts of Interest: The authors declare no conflict of interest.

References

- Ogoshi, T.; Yamagishi, T.; Nakamoto, Y. Pillar-shaped macrocyclic hosts pillar[n]arenes: New key players for supramolecular chemistry. *Chem. Rev.* **2016**, *116*, 7937–8002. [[CrossRef](#)]
- Vinodh, M.; Alipour, F.H.; Al-Azemi, T.F. Spatially designed supramolecular anion receptors based on pillar[5]arene scaffolds: Synthesis and halide anion binding properties. *ACS Omega* **2023**, *8*, 1466–1475. [[CrossRef](#)]
- Al-Azemi, T.F.; Vinodh, M. External-stimulus-triggered conformational inversion of mechanically self-locked *pseudo*[1] catenane and *gemini*-catenanes based on A1/A2- alkyne–azide-difunctionalized pillar[5]arenes. *RSC Adv.* **2022**, *12*, 1797–1806. [[CrossRef](#)] [[PubMed](#)]
- Gomez, B.; Francisco, V.; Fernandez-Nieto, F.; Garcia-Rio, L.; Martin-Pastor, M.; Paleo, M.R.; Sardina, F.J. Host-guest chemistry of a water-soluble pillar[5]arene: Evidence for an ionic-exchange recognition process and different complexation modes. *Chemistry* **2014**, *20*, 12123–12132. [[CrossRef](#)]
- Li, Z.Y.; Zhang, Y.; Zhang, C.W.; Chen, L.J.; Wang, C.; Tan, H.; Yu, Y.; Li, X.; Yang, H.B. Cross-linked supramolecular polymer gels constructed from discrete multi-pillar[5]arene metallacycles and their multiple stimuli-responsive behavior. *J. Am. Chem. Soc.* **2014**, *136*, 8577–8589. [[CrossRef](#)] [[PubMed](#)]

6. Al-Azemi, T.F.; Vinodh, M. Pillar[5]arene-based self-assembled linear supramolecular polymer driven by guest halogen–halogen interactions in solid and solution states. *Polym. Chem.* **2020**, *11*, 3305–3312. [[CrossRef](#)]
7. Li, M.; Liu, Y.; Shao, L.; Hua, B.; Wang, M.; Liang, H.; Khashab, N.M.; Sessler, L.L.; Huang, F. Pillararene-Based Variable Stoichiometry Co-Crystallization: A Versatile Approach to Diversified Solid-State Superstructures. *J. Am. Chem. Soc.* **2023**, *145*, 667–675. [[CrossRef](#)] [[PubMed](#)]
8. Eichstaedt, K.; Wicher, B.; Gdaniec, M.; Połonki, T. Halogen bonded polypseudorotaxanes based on a pillar[5]arene host. *CrystEngComm* **2016**, *18*, 5807–5810. [[CrossRef](#)]
9. Mukherjee, A.; Tothadi, S.; Desiraju, G.R. Halogen bonds in crystal engineering: Like hydrogen bonds yet different. *Acc. Chem. Res.* **2014**, *47*, 2514–2524. [[CrossRef](#)]
10. Liu, P.R.; Li, Z.T.; Shi, B.B.; Liu, J.Y.; Zhu, H.T.Z.; Huang, F.H. Formation of linear side-chain polypseudorotaxane with supramolecular polymer backbone through neutral halogen bonds and pillar[5]arene-based host–guest interactions. *Chem. Eur. J.* **2018**, *24*, 4264–4267. [[CrossRef](#)]
11. Vinodh, M.; Al-Azemi, T.F. Linear supramolecular polymer driven by Br···Br and Br···H non-bonding interactions based on inclusion-complex of octabromo-functionalized pillar[a]rene. *J. Chem. Cryst.* **2022**, *52*, 399–406. [[CrossRef](#)]
12. Han, C.; Zhaoa, D.; Dong, S. Three-dimensional supramolecular polymerization based on pillar[n]arenes ($n = 5, 6$) and halogen bonding interactions. *Chem. Commun.* **2018**, *54*, 13099–13102. [[CrossRef](#)] [[PubMed](#)]
13. Popa, M.M.; Shova, S.; Dascalu, M.; Caira, M.R.; Dumitrescu, F. Crystal structures of 5-bromo-1-arylpypyrazoles and their halogen bonding features. *CrystEngComm* **2023**, *25*, 86–94. [[CrossRef](#)]
14. Adonin, S.A.; Bondarenko, M.A.; Novikov, A.S.; Abramov, P.A.; Plyusnin, P.E.; Sokolov, M.N.; Fedin, V.P. Halogen bonding-assisted assembly of bromoantimonate(v) and polybromide-bromoantimonate-based frameworks. *CrystEngComm* **2019**, *21*, 850–856. [[CrossRef](#)]
15. Adonin, S.A.; Bondarenko, M.A.; Novikov, A.S.; Sokolov, M.N. Halogen bonding in isostructural Co(II) complexes with 2-halopyridines. *Crystals* **2020**, *10*, 289. [[CrossRef](#)]
16. Aschi, M.; Brocchi, G.T.; Portalone, G. A combined experimental and computational study of halogen and hydrogen bonding in molecular salts of 5-bromocytosine. *Molecules* **2021**, *26*, 3111. [[CrossRef](#)]
17. Baykov, S.V.; Presnukhina, S.I.; Novikov, A.S.; Shetnev, A.A.; Boyarskiy, V.P.; Kukushkin, V.Y. 2,5-Dibromothiophenes: Halogen bond involving packing patterns and their relevance to solid-state polymerization. *Cryst. Growth Des.* **2021**, *21*, 2526–2540. [[CrossRef](#)]
18. Easton, M.E.; Chan, B.; Masters, A.F.; Radom, L.; Maschmeyer, T. Beyond the halogen bond: Examining the limits of extended polybromide networks through quantum-chemical investigations. *Chem. Asian J.* **2016**, *11*, 682–686. [[CrossRef](#)] [[PubMed](#)]
19. Vologzhanina, A.V.; Buikin, P.A.; Alexander, A.; Korlyukov, A.A. Peculiarities of Br···Br bonding in crystal structures of polybromides and bromine solvates. *CrystEngComm* **2020**, *22*, 7361–7370. [[CrossRef](#)]
20. Levina, E.O.; Chernyshov, I.Y.; Voronin, A.P.; Alekseiko, L.N.; Stash, A.I.; Mikhail, V.; Vener, M.V. Solving the enigma of weak fluorine contacts in the solid state: A periodic DFT study of fluorinated organic crystals. *RSC Adv.* **2019**, *9*, 12520–12537. [[CrossRef](#)]
21. Chopra, D. Is organic fluorine really “not” polarizable? *Cryst. Growth Des.* **2012**, *12*, 541–546. [[CrossRef](#)]
22. Hu, W.B.; Hu, W.J.; Zhao, X.L.; Liu, Y.A.; Li, J.S.; Jiang, B.; Wen, K. A1/A2-diamino-substituted pillar[5]arene-based acid-base-responsive host–guest system. *J. Org. Chem.* **2016**, *81*, 3877–3881. [[CrossRef](#)]
23. Al-Azemi, T.F.; Mohamod, A.A.; Vinodh, M.; Alipour, F.H. A new approach for the synthesis of mono- and A1/A2-dihydroxy-substituted pillar[5]arenes and their complexation with alkyl alcohols in solution and in the solid state. *Org. Chem. Front.* **2018**, *5*, 10–18. [[CrossRef](#)]
24. Spackman, A.M.; Jayatilaka, D. Hirshfeld surface analysis. *CrystEngComm* **2009**, *11*, 19–32. [[CrossRef](#)]
25. McKinnon, J.J.; Spackman, M.A.; Mitchell, A.S. Novel tools for visualizing and exploring intermolecular interactions in molecular crystals. *Acta Cryst. B* **2004**, *60*, 627–668. [[CrossRef](#)]
26. McKinnon, J.J.; Jayatilaka, D.; Spackman, M.A. Towards quantitative analysis of intermolecular interactions with Hirshfeld surfaces. *Chem. Commun.* **2007**, *37*, 3814–3816. [[CrossRef](#)]
27. Turner, M.J.; McKinnon, J.J.; Wolff, S.K.; Grimwood, D.J.; Spackman, P.R.; Jayatilaka, D.; Spackman, A.M. *CrystalExplorer17*; University of Western Australia: Perth, Australia, 2017; Available online: <https://hirshfeldsurface.net> (accessed on 10 March 2023).

Disclaimer/Publisher’s Note: The statements, opinions and data contained in all publications are solely those of the individual author(s) and contributor(s) and not of MDPI and/or the editor(s). MDPI and/or the editor(s) disclaim responsibility for any injury to people or property resulting from any ideas, methods, instructions or products referred to in the content.